Proximity Relationships and Structural Dynamics of the Phalloidin Binding Site of Actin Filaments in Solution and on Single Actin Filaments on Heavy Meromyosin†

Manfred Heidecker, Yuling Yan-Marriott, and Gerard Marriott*

Biomolecular and Cellular Dynamics Research Group, Max Planck Institute for Biochemistry, Am Klopferspitz 18a, 82152 Martinsried, Germany

Received February 20, 1995; Revised Manuscript Received May 23, 1995®

ABSTRACT: Distance relationships between phalloidin binding sites on F-actin have been investigated using fluorescence resonance energy transfer (FRET) techniques in solution and on single F-actin filaments bound to heavy meromyosin (HMM). Filaments saturated with an equimolar concentration of fluoresceinisothiocyanatophalloidin (FITC-ph) as the donor and tetramethylrhodamineisothiocyanatophalloidin (TRITC-ph) as the acceptor and control filaments saturated with either FITC-ph or TRITC-ph were characterized by absorption and fluorescence spectroscopy and the in vitro motility assay. Fluorescence excitation polarization spectroscopy showed hetero-FRET occurred within colabeled filaments, whereas homo-FRET was observed in control filaments. The distance measured between adjacent phalloidin binding sites using randomly labeled FITC-ph and TRITC-ph was 37.2 Å using steady-state spectral analysis and 36.9 Å using time-resolved spectroscopy with a radial coordinate of 14.5 Å. Measurements of the distance between fluorescent phalloidin groups using the atomic model of F-actin [Lorenz, M., Popp, D., & Holmes, K. C. (1993) *J. Mol. Biol. 234*, 826−836] suggest transfer occurs between adjacent phalloidin molecules on opposite actin helices (39 Å), rather than between adjacent phalloidins along the same actin helix (55.4 Å). A quantitative fluorescence microscope technique was described that measures the proximity of adjacent FITC-ph and TRITC-ph on single filaments immobilized on HMM. Here a distance of 36.2 Å was calculated which was unchanged during ATP-dependent sliding of F-actin on HMM. Spatially resolved FRET measurements are being used to observe the effects of actin binding proteins on the structural properties along the length of single actin filaments.

The X-ray crystal structure of the DNase−G-actin complex (Kabsch et al., 1990) and subsequent modeling of the F-actin filament structure (Holmes et al., 1990) provides essential information for studies of the structure, function, dynamics, and regulation of actin filaments. The structure and structural dynamics of the actin filament are influenced by the interaction of ligands, e.g., ATP vs ADP and actin binding proteins (ABPs; Janmey et al., 1990), and modulation of the physical properties of the filament or filament network may be relevant to the mechanism of force transduction in motile cells. Förster-type fluorescence resonance energy transfer (FRET) techniques are well suited to study proximity relationships, structural dynamics, and molecular interactions between actin filaments and ABPs (Miki et al., 1992). FRET between a fluorescent donor (D) and fluorescent or nonfluorescent acceptor (A) molecule will occur if the following conditions are satisfied: (1) the D−A distance is between 10 and 100 Å, (2) a reasonable spectral overlap exists between the emission spectrum of the donor and the absorption spectrum of the acceptor, and (3) the angle between the emission and absorption oscillators is other than 90° (Förster, 1948). Most of these FRET conditions are satisfied for adjacent actin monomers in the actin filament, as well as between the actin monomer and ABPs [for a review, see Miki et al. (1992)]. For example, Taylor et al. [1981; followed up by later studies (Kasprzrak et al., 1988; Moens et al., 1994)] measured FRET between actin monomers labeled at cysteine-374 in F-actin and calculated a distance of 57 Å, consistent with the atomic model of F-actin (Holmes et al., 1990). On the other hand, multiple labeling sites and substoichiometric labeling are probably responsible for other distances measured by FRET that are widely different from Holmes' structure [reviewed by Miki et al. (1992)].

In the first part of this paper we investigate the distance relationships between adjacent fluorescent phalloidin binding sites of F-actin using FRET and present a detailed account of the spectroscopic behavior of fluorescent phalloidins on filaments using fluorescence polarization spectroscopy. The phalloidin binding site is an excellent site to probe proximity relationships and structural dynamics of the actin filament for the following reasons: (1) this site is located at the interface of three actin monomers close to the helix axis (Barden et al., 1987) and as such is expected to be sensitive to changes of the structure and dynamics of the filament that might occur during the ATP-dependent sliding of actin filaments on myosin or upon the interaction with ABPs; (2) phalloidin and its fluorescent derivatives bind reversibly to F-actin with high affinity and a stoichiometry of phalloidin: actin monomer of 1:1 and have an off-rate of about 90 min (Wülf et al., 1979; Huang et al., 1991; Marriott, unpublished results); and (3) fluorescent phalloidins are used extensively in microscopy to stain actin filaments in vivo (Wülf et al., 1979) and to visualize single F-actin filaments on a surface

† This work was supported by a grant from the Max Planck Society (Ma-215).

* To whom correspondence should be addressed (telephone, +49 89 85 78 23 14; Fax, +49 89 85 78 3777; e-mail, Marriott @vms.biochem.mpg.de).

® Abstract published in *Advance ACS Abstracts,* August 29, 1995.

0006-2960/95/0434-11017$09.00/0

of HMM (Kron et al., 1991). In the second part of this paper we show how fluorescence microscopic techniques can be used to study proximity relationships of fluorescent phalloidins bound to single actin filaments. Intuitively, ratio-based quantitative microscopic techniques that measure the efficiency of FRET (Xue et al., 1992) are best suited to study molecular interactions, molecular distances, and the structural dynamics of single actin filaments. However, previous studies have shown that quantitative FRETIM employing steady-state fluorescence emission detection is complicated because of the inability to compare donor emission in the absence and presence of acceptor in the same image field and problems of image registration for diffusing samples. To overcome these problems, we have used the actin–myosin-based in vitro motility assay in which fluorescent phalloidin-labeled actin filaments containing either only donor, acceptor, and donor–acceptor were imaged in the same field in the rigor complex and during ATP-dependent sliding on HMM.

MATERIALS AND METHODS

Absorption measurements were made in a HP 8452 diode-array spectrophotometer; fluorescence measurements were conducted in a SLM AB2 fluorescence spectrophotometer (SLM, Urbana, IL) at 19 °C unless otherwise noted. Steady-state excitation and emission spectra (2 or 4 nm bandpass) were measured with magic angle excitation and corrected for the detection response of the instrument (Marriott et al., 1988). Steady-state excitation polarization spectra were recorded in an L-format configuration. Excitation polarization spectra provide important information on homo-FRET (Anderson & Weber, 1969; Marriott et al., 1988) and hetero-FRET. FRET is easily recognized in the spectrum by the decrease in the polarization value of the donor when monitored at a sensitized emission wavelength (hetero-FRET) or by the decrease in the polarization value when monitored at the donor emission wavelength (homo-FRET).

Time-resolved fluorescence intensity decay measurements of actin filaments labeled with fluorescent phalloidins were kindly performed by Prof. Peter Fromhertz and Martin Leonhard of this Institute. Magic angle excitation of the FITC-ph was made at 450 nm with 2 ps pulses delivered by an argon ion/Tsunami laser (Spectra Physics) operating at 4 MHz. An emission wavelength of either 530 or 600 nm was selected using a double monochromotor. Decay rates were calculated using the data analysis program IGOR running on a Macintosh IIfx.

Proteins and Protein Labeling

Muscle Proteins. Actin and myosin were purified from rabbit leg muscle. The animal was narcotized and desauget-ized, and the leg muscle was rapidly excised and chilled on ice for 30 min. The following steps were performed in the cold room: the muscle was weighed (1 volume) and twice minced in a precooled meat mincer and extracted by gentle stirring for 10 min in 3 volumes of Guba–Straub solution (0.3 M KCl, 0.15 M KH_2PO_4, pH 6.4 at 25 °C) at −4 °C. The suspension was centrifuged at 5000*g* at 2 °C for 10 min. The pellet was used to prepare acetone powder according to Pardee and Spudich (1982), while the supernatent was used to isolate the myosin following a method described by Kinosita et al. (1991) with the slight modification that EDTA was added to 0.1 mM and β-mercaptoethanol to 2 mM in the first cold water precipitation of crude myosin. HMM was produced from myosin by chymotryptic digestion using a ratio of myosin to α-CHT of 800/1 by weight for 8 min at 25 °C. Proteolysis was terminated by the addition of PMSF to 0.5 mM, and it was also included in the dialysis buffer to 50 μM.

F-Actin was purified from rabbit muscle according to Spudich and Watt (1971) and stored as F-actin in AB buffer (25 mM imidazole, 25 mM KCl, 1.0 mM DTT, 4 mM $MgCl_2$, pH 7.4) or F-buffer (5 mM Tris, 0.2 mM ATP, 0.2 mM $CaCl_2$, 1 mM DTT, pH 8.0). The concentration of G-actin was calculated using an extinction coefficient at 290 nm of 0.63 mg/mL (Gordon et al., 1976). FITC-ph and TRITC-ph with extinction coefficients of 72 000 and 85 000 $M^{-1}\cdot cm^{-1}$, respectively (Waggoner et al., 1989), were purchased from Fluka and dissolved in methanol (Fluka, puriss) to 1 mg/mL. Filaments containing a stoichiometric amount of either FITC-ph or TRITC-ph were prepared by adding 1.5 equiv of fluorescent phalloidin over the actin monomer concentration (10 μM) in the filament. Colabeled filaments were prepared by adding 0.75 equiv of each phalloidin, with respect to the G-actin concentration in the filament, to prepolymerized F-actin. The final volume of methanol was always below 1%. Fluorescently labeled F-actin samples (10 μM) were left overnight at 4 °C or longer to allow for complete saturation of binding sites. Excess dye was removed by centrifuging the fluorescent filaments at 100000*g* for 60 min, followed by resuspension of the pellet in AB buffer or F-buffer. The next day the pellet was diluted in AB buffer and analyzed by absorption spectrophotometry and fluorescence spectroscopy to determine the degree of labeling. These actin filaments were found to be stable for several weeks as monitored by their maximum sliding velocity (4–5 μm/s) on HMM using the in vitro motility assay.

In Vitro Motility Assay. A hybrid protocol based on Kron et al. (1991) and Kinosita et al. (1991) was used to observe fluorescent actin filaments in rigor or during ATP-dependent sliding on an HMM-covered surface. A flow-through chamber was constructed which consists of a large coverslip (25 × 50 mm) separated from a smaller one (24 × 24 mm) by spacers made from greased strips of parafilm paper. The large coverslips had been previously washed in 10% HCl and absolute ethanol, dried under an N_2 stream, and stored or used with the following steps: sonication in 0.1 M KOH for 30 min, washing in ethanol, drying under a stream of nitrogen, and coating with nitrocellulose (Electron Microscopy Sciences) diluted to 0.1% in isoamyl acetate. The chamber was flushed with protein solutions and buffers as described previously (Kron et al., 1991) except that BSA and EDTA were not included in the AB buffer. F-Actin filaments were imaged within a few minutes of the final wash buffer to limit the dissociation of phalloidin molecules.

Microscope Instrumentation. A schematic of the microscope workstation used in these studies is shown in Figure 1. Excitation was made with an mercury arc lamp and the excitation wavelength selected with an interference filter (450–480 nm). A dichroic mirror was used (Zeiss, Oberkochen) to reflect the excitation and transmit the emission (>500 nm) which was selected with either an interference filter with transmittance between 515 and 565 nm or a cutoff filter with a 50% transmission at 520 nm for

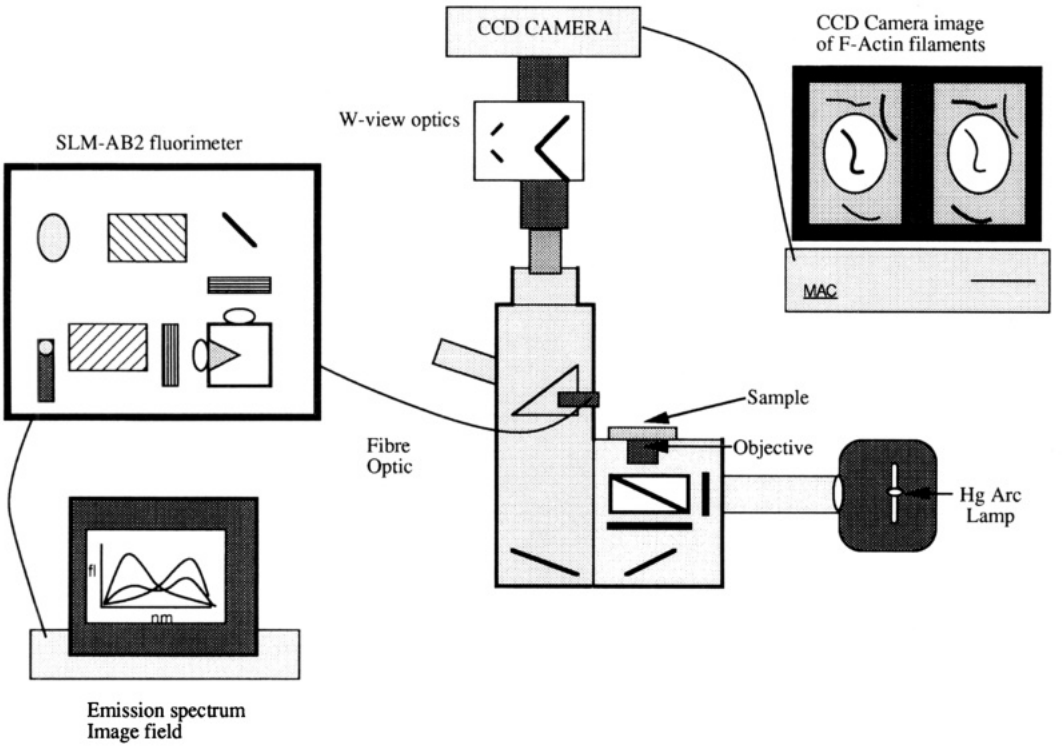

FIGURE 1: Schematic of the fluorescence microscope (details in text) used in these studies to observe simultaneous images of the tetramethylrhodamine and fluorescein emissions using the W-view microscope adaptor. Splitting the image off to a fluorometer with a fiber optic makes it possible to simultaneously acquire fluorescence spectra of the image field.

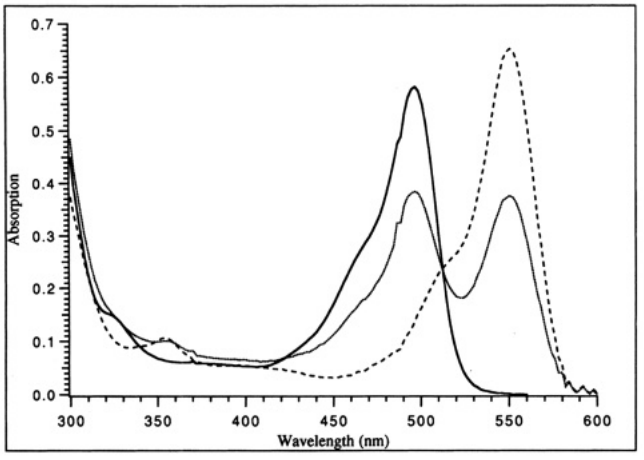

FIGURE 2: Absorption spectra of 7.97 μM FITC-ph-labeled actin filaments (solid line), 4.44 μM FITC-ph/4.46 μM TRITC-ph- (1:1) labeled actin filaments (dotted line), and 7.65 μM TRITC-ph-labeled actin filaments (dashed line) in AB buffer.

double-view microscopy. A Fluar objective (100×, 1.3 NA; Zeiss) was employed in all the studies reported herein. There are a couple of different methods to image and quantitate FRET on single fluorescently labeled actin filaments in the microscope. The first is to image, in the same field, the relative quantum yield of the donor emission (FITC-ph) in the absence and presence of acceptor (TRITC-ph) using an excitation filter that is biased for the donor absorption spectrum (450−480 nm) and an emission filter that transmits the donor emission (515−565 nm). The second method employs selective excitation of the donor and simultaneous imaging of the FITC-ph and TRITC-ph emission using the Kinosita "W-view" adaptor (Kinosita et al., 1991). In both cases image acquisition times were typically 2−5 s. For W-view imaging the image emerging from the microscope is made parallel and passes through the W-view adaptor. The dichroic mirrors of the W-view adaptor transmit light between 515 and 565 nm and reflect light beyond 580 nm. An adjustable slit device was constructed and located at the intermediate image of the Zeiss Axiovert 35 microscope: this device serves to separate and adjust the field of the two images. The two images were focused onto either a Photometrics cooled CCD (Nu200 series) operating under control of a Macintosh Quadra 650 computer or a Hamamatsu ICCD camera, in which case video rate images were stored on a Super-VHS video tape or else captured using a Scion LG3 frame grabber (Scion Inc., Frederick, MD) with 16 MB of memory on board. After a careful initial positioning of the lenses and mirrors of the W-view adaptor, little readjustment was found necessary: the two images of the filaments were always in focus and the same size. FRET was also measured between fluorescent phalloidins on single actin filaments by microspectrofluorometry. In this case the emission image was split 30/70 before the W-view adaptor and 30% of the emission image directed via a 4 mm diameter 6 m long quartz fiber optic cable into the optical module of an SLM-AB2 spectrofluorometer (Urbana, IL) for fluorescence spectrometry. W-view FRETIM with simultaneous spectral analysis was normally performed on an image field containing several tens of fluorescent actin filaments, although we have recorded the emission spectrum and the fluorescence image of a single 5 μm actin filament labeled with TRITC-ph (data not shown).

Digital Image Processing

Images of fluorescence and rhodamine emission obtained by single wavelength observation or W-view fluorescence microscopy were analyzed using the Nu200 software (Photometrics) or NIH image.

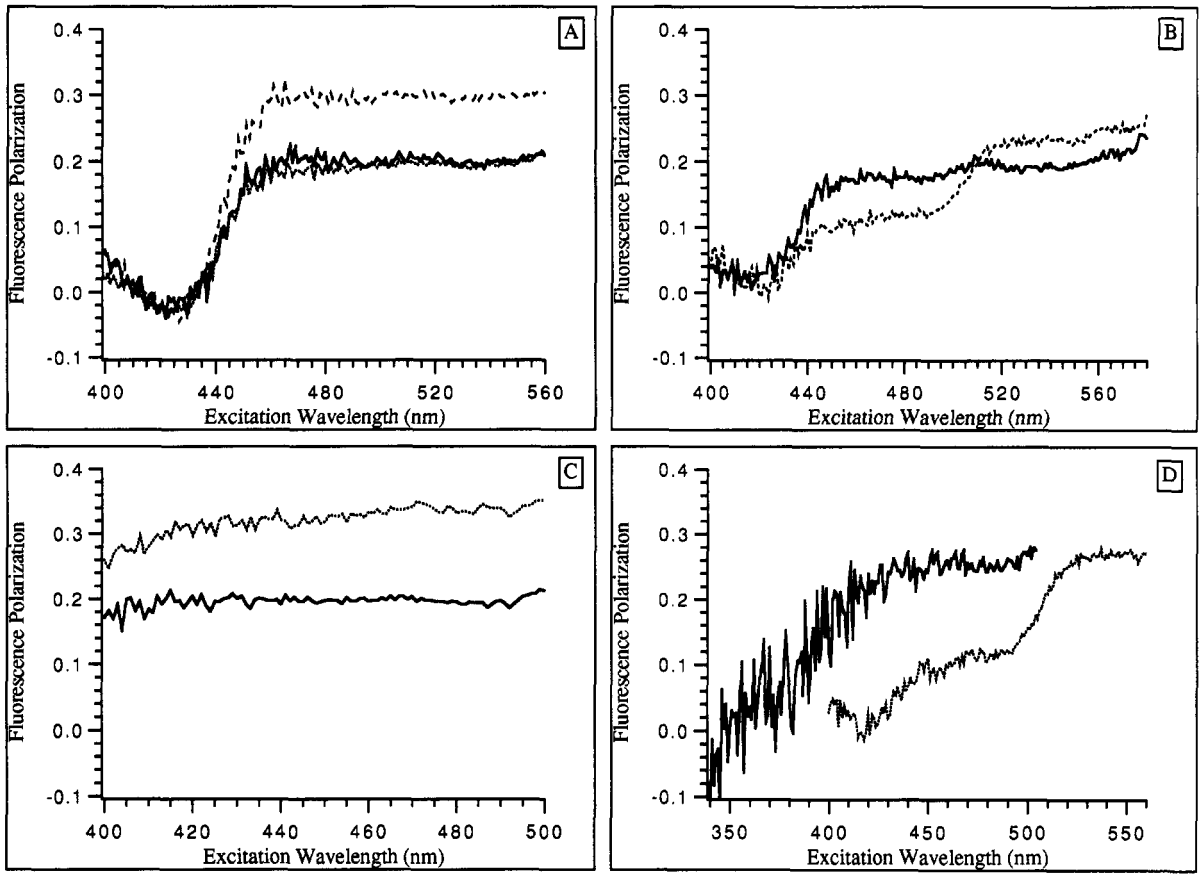

FIGURE 3: (A) Excitation polarization spectra of TRITC-ph-labeled F-actin, 1.91 μM (solid line), 3.82 μM (dotted line), and 1.91 μM, in the presence of 6 μM unlabeled F-actin (dashed line). Excitation bandpass was at 2 nm and emission at 580 nm. (B) Excitation polarization spectra of 3.99 μM FITC-ph-labeled F-actin and 3.82 μM TRITC-ph-labeled F-actin (solid line) after 1 min of mixing and (dotted line) after 1 h of mixing. Emission wavelength was 580 nm. (C) Excitation polarization spectra of 1.53 μM FITC-ph-labeled F-actin in AB buffer at 20 °C (solid line) and 1.53 μM FITC-ph-labeled F-actin in 80% glycerol/AB buffer at 2 °C (dotted line). Emission wavelength was 530 nm. (D) Excitation polarization spectra of 1.99 μM FITC-ph/1.91 μM TRITC-ph-labeled F-actin with emission at 530 (solid line) and at 600 nm (dotted line).

RESULTS

Spectroscopic Characterization of FITC-ph- and TRITC-ph-Labeled Filaments in Solution. The absorption spectrum of the three types of fluorescent phalloidin-labeled actin filaments, prepared according to the Materials and Methods section, is shown in Figure 2. The labeling ratio, expressed in terms of actin monomer to fluorescent phalloidin, was determined from the absorption spectra following correction of the absorption value of FITC-ph at 492 nm for the contribution of TRITC-ph. Control experiments were performed to show the decrease in the FITC-ph intensity in the presence of the acceptor was due to nonradiative FRET and not a result of trivial causes of donor quenching. (1) The fluorescence intensity originating from stoichiometrically bound FITC-ph (or TRITC-ph) was linear with the degree of saturation and so independent of the degree of occupancy, which rules out fluorescein (or rhodamine) quenching through adjacent site occupancy (data not shown; Huang et al., 1991). (2) Trivial reabsorption of the fluorescence does not occur if the optical density of the solution is below 0.2 unit at the maximum absorption wavelength of the dye. We confirmed this by measuring fluorescence excitation polarization spectra of FITC-ph filaments, TRITC-ph filaments, and FITC-ph/TRITC-ph-colabeled filaments as a function of the optical density of the solution. No change in the polarization value monitored at 580 nm was found for TRITC-ph F-actin at a concentration of 3.82 or 1.91 μM (Figure 3A) when measured in a 3 × 3 mm cuvette. Similarly, no significant difference was found in the FRET efficiency for these two concentrations (data not shown). (3) That FRET is restricted to fluorescent phalloidins within the same filament and not a result of trivial reabsorption effects was shown by recording the excitation polarization spectrum of filaments labeled with either FITC-ph or TRITC-ph that had been gently mixed in the same cuvette (Figure 3B). A time-dependent increase in FRET efficiency was apparent after 1 h at 18 °C, as measured by the decrease in the polarization value of FITC-ph measured between 450 and 490 nm using detection of the sensitized emission at 570 nm. This time-dependent increase in FRET is due to an exchange of a certain population of fluorescent phalloidins between filaments and not a result of interchange of actin monomers between filaments, since Taylor et al. (1981) have shown that the rate of monomer exchange between filaments is slow for undisturbed samples. FRET, as manifested in the excitation polarization spectrum, is more strikingly seen for a completely randomized distribution of fluorescent phalloidins on F-actin shown in Figure 3D. The effect of hetero-FRET on the depolarization of FITC-ph fluorescence can also be seen in the excitation polarization spectrum of colabeled filaments compared to pure FITC-ph-labeled filaments (Figure 3C) when the emission is monitored at

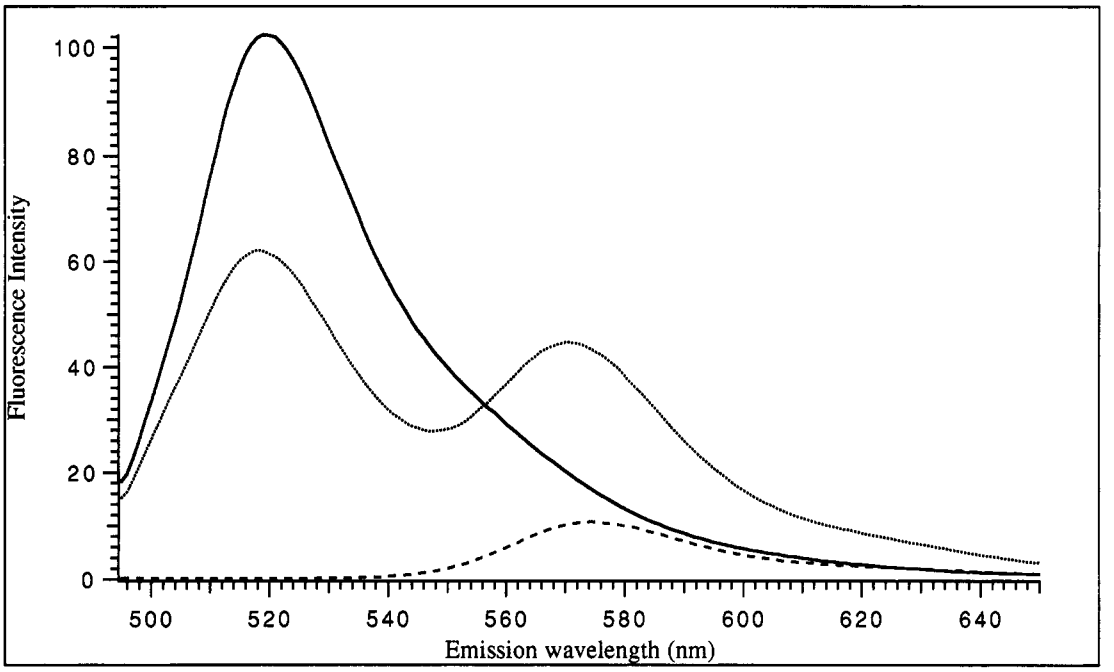

FIGURE 4: Steady-state, corrected fluorescence emission spectrum of FITC-ph-labeled F-actin, normalized to 4.44 μM (solid line), and steady-state, corrected fluorescence emission spectrum of 4.44 μM FITC-ph/4.46 μM TRITC-ph-labeled F-actin (dotted line) corrected for indirect excitation of TRITC-ph (dashed line). Excitation wavelength was 488 nm with a 2 nm bandpass.

either 530 nm (higher polarization value, no FRET; Figure 3D) or 580 nm (lower polarization value, sensitized emission; Figure 3D). In FITC-ph filaments local motion of the probe contributes to the depolarization of the fluorescence since the polarization value of FITC-ph F-actin in 80% glycerol at 2 °C is significantly higher than in aqueous buffer as a result viscosity damping (Figure 3C).

Homo-FRET is also responsible for the relatively low polarization value found for the fluorescent phalloidin filaments, as can be seen in the excitation polarization spectrum of TRITC-ph-labeled filaments measured in the absence or presence of 6 μM unlabeled F-actin (Figure 3A). The higher polarization value observed for the sample with excess unlabeled F-actin results from an exchange of TRITC-ph to the unlabeled filaments, thereby decreasing the probability of finding two TRITC-ph molecules on adjacent sites (the R_0 for homo-FRET between FITC−FITC is about 40 Å). Homo-FRET can also be inferred from the higher polarization value found for direct excitation of TRITC-ph in colabeled filaments (Figure 3D) compared to pure TRITC-ph filaments (Figure 3A), as well as for direct excitation and observation of FITC-ph emission in colabeled filaments (Figure 3D) compared to pure FITC-ph-labeled filaments (Figure 3C). Again these effects result from the lower probability of finding adjacent homotransfer pairs (25%) in the colabeled filaments compared to that in pure FITC-ph-labeled filaments (100%). The existence of homo-FRET in fluorescent phalloidin-labeled actin filaments has important consequences in FPIM investigations of the orientation of phalloidin on single actin filaments (Kinosita et al., 1991; Borejo & Burlaca, 1994). We argue that the homo-FRET seen in filaments saturated with either TRITC-ph or FITC-ph results in an underestimate of the polarization value when measured on single filaments, which leads to an overestimate of the inferred angle the phalloidin group makes with the filament axis [30−40° as reported by Kinosita et al. (1991) and Borejo and Burlaca (1994)].

Quantum Yield Determination of FRET. The efficiency of FRET was measured by observing the decrease in the relative quantum yield of FITC-ph on filaments colabeled (1:1) with TRITC-ph, compared to filaments labeled with FITC-ph alone as calculated from the integrated, corrected emission spectrum (Figure 4). Since most measurements were made in a microcuvette (3 mm × 3 mm), a concentration of labeled F-actin of 5−10 μM could be used without incurring inner filter effects. The wavelength-dependent fluorescence emission intensity of the colabeled sample was first normalized in terms of the concentration of FITC-ph on the filament. The spectra were then corrected to account for the equilibrium concentration of free FITC-ph and free TRITC-ph. The contribution to the emission from free FITC-ph and/or free TRITC-ph was calculated on the basis of the equilibrium concentration which was determined by separately recording the emission intensity of the supernatent fraction of FITC-ph filaments (or TRITC-ph filaments) before and after centrifugation at 100000g for 1 h. In the case of FITC-ph filaments 4.7% of the emission was found in the supernatent fraction from which we arrive at an approximate K_d of 0.36 μM. The spectrum shown in Figure 4 was also corrected for direct excitation of TRITC-ph (normalized concentration) with 488 nm excitation.

Förster (1948) derived on the basis of a quantum mechanical consideration the rate of energy transfer between a donor and acceptor which is given by

$$k_t = 1/\tau(8.79 \times 10^{-5})(K^2 n^4 \Phi_d J_{da} R^{-6})$$

where k_t is the rate of energy transfer, τ is the fluorescence lifetime of the donor, K^2 is the orientation factor between the filaments, n is the refractive index of the medium, Φ_d is the quantum yield of the donor, J_{da} is the spectral overlap integral between the donor emission and the acceptor absorption spectrum, and R is the distance in angstroms between the donor and acceptor molecules. The efficiency

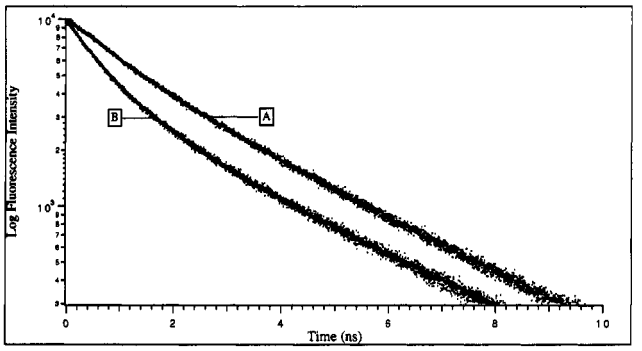

FIGURE 5: Time-resolved fluorescence intensity decays of a 7.97 μM solution of FITC-ph-labeled F-actin (A) and a solution of 4.44 μM FITC-ph/4.46 μM TRITC-ph-labeled F-actin (B). The excitation wavelength in both samples was 450 nm, and emission was at 530 nm.

of FRET was computed using the relationship

$$E_t = (1 - \Phi_{da}/\Phi_d)$$

The measured transfer efficiency value of 0.408 is based on the assumption that every FITC-ph bound to the filament (colabeled 1:1 with TRITC-ph) is capable of undergoing energy transfer with its adjacent TRITC-ph molecule. However, a statistical evaluation of randomly labeled sites shows that only three in four FITC-ph molecules satisfy this condition, leading to a revised transfer efficiency of E_t = 0.51.

The rate of transfer (k_t) is related to the energy-transfer efficiency (E_t) according to the expression

$$E_t = k_t/k_t + k_f + {}_{ki}$$

where k_f is the rate of fluorescence emission of the donor and k_i is the rate of other deactivating processes of the excited state of the donor; these processes are the same for FITC-ph filaments and colabeled filaments. The average fluorescence lifetime of FITC-ph bound to actin filaments is 1.44 ns (Figure 5; $k_f = 7.0 \times 10^8$ s^{-1}) or a k_t of 7.29×10^8 s^{-1}.

The angular dependence of the dipole−dipole energy transfer, the K^2 value, is given by

$$K^2 = (\cos \alpha - 3 \cos \beta \cos \gamma)^2$$

where α is the angle between the donor and acceptor transition moments, β is the angle between the donor moment and the line adjoining the centers of the donor and acceptor, and γ is the angle between the acceptor moment and the line joining the centers of the donor and acceptor (Fairclough & Cantor, 1978). The K^2 value for adjacent fluorescent phalloidins in the filament was calculated by considering the spatial and angular relationship of the binding site in the actin filament. Thus each monomer in the filament is related to its neighbor by an axial translation of 2.75 nm and a rotation of 166° (Taylor et al., 1981). Furthermore, given a radial coordinate of the fluorescent phalloidin of 1.45 nm (see below) and the angle the donor/acceptor makes with the helix axis of 30° (Kinosita et al., 1991), we calculate a K^2 value of 1.42. The difference between the distance calculated using this K^2 value, which assumes the fluorophore maintain the same orientation on the fluorescence time scale, and the random orientation value of 0.67 is only 13%. Our steady-state polarization data combined with time-resolved anisotropy measurements of FITC-ph F-actin filaments (data not shown) indicate that the donor molecule has a fast rotation with a correlation time of 0.3 ns, which would tend to randomize the orientations of the donor and acceptor. For this reason we have chosen to use the random orientation value of K^2 of $^2/_3$ in our calculations. The refractive index was taken as 1.4 (Fairclough & Cantor, 1978). The quantum yield of FITC-ph-labeled filaments (Φ = 0.37) was determined by comparing the corrected, integrated emission spectrum of an exact concentration (measured by absorption) of the labeled filaments with the corrected, integrated emission spectrum of a solution of disodium fluorescein in 0.01 M NaOH (with a quantum yield of 0.91) with the same optical density as the labeled filaments at the maximum wavelength (Fairclough & Cantor, 1978).

The value of the spectral overlap integral J_{da} of 4.9×10^{14} M^{-1}·cm^{-1}·nm^4 was calculated using the expression

$$J_{da} = \int F_d(\lambda)\, \epsilon_a(\lambda)\, \lambda^4\, d\lambda / \int F_d(\lambda)\, d\lambda$$

using the corrected and normalized emission spectrum of FITC-ph-labeled filaments; ϵ, the molar absorptivity of TRITC-ph-labeled filaments as a function of wavelength, is based on a value at 552 nm of 85 000 M^{-1}·cm^{-1} (Waggoner et al., 1989). The distance calculated between the fluorescent phalloidins using the decrease in the quantum yield and Förster theory is 37.2 Å, with an R_0 of 37.4 Å.

Time-Resolved Intensity Decay. The fluorescence lifetime of FITC-ph filaments and FITC-ph filaments containing an equal concentration of TRITC-ph was measured with excitation at 450 nm and emission at 530 nm. Calculation of the distance using fluorescence lifetime analysis is independent of the labeling ratio. The decay profiles were analyzed in terms of double-exponential decays and are shown in Figure 5. For FITC-ph-labeled filaments we obtained the following fit: τ_1 = 1.29 ns, f_1 = 0.89, τ_2 = 3.3 ns; for colabeled filaments, we obtained τ_1 = 0.667 ns, f_1 = 0.99, τ_2 = 3.2 ns. The average lifetime values (1.44 and 0.69 ns) were used in calculating the FRET efficiency using the relationship

$$E_t = (1 - \tau_{da}/\tau_d) = 0.52$$

from which the rate of transfer (k_t) was calculated to be 7.58×10^8 s^{-1}. Workup of the Förster equation using the values described in the previous section gave a calculated distance between adjacent phalloidin binding sites of 36.9 Å, which is in good agreement with the value obtained from steady-state spectral analysis. A radial coordinate of 14.5 Å was calculated from the distance calculated between phalloidin molecules on opposite actin helices using the approach described by Taylor et al. (1981).

We introduced the FITC and TRITC molecules into the molecular model of the phalloidin-labeled actin filament (Lorenz et al., 1993; Figure 6) in an effort to better define the distance between the fluorophores attached to phalloidin, as it is unlikely that the bound FITC-ph and TRITC-ph have the same radial coordinate as the hydroxyleucine atom of phalloidin, which is 32.3 Å apart on adjacent phalloidin binding sites on opposite actin helices and more than 55 Å apart between the same atom along the same actin helix (Lorenz et al., 1993). Using the center of the xanthine ring as a reference point, we find the distance between adjacent fluorophores on opposite helices is 39 Å, which, considering the large size of the probe molecules, agrees well with the

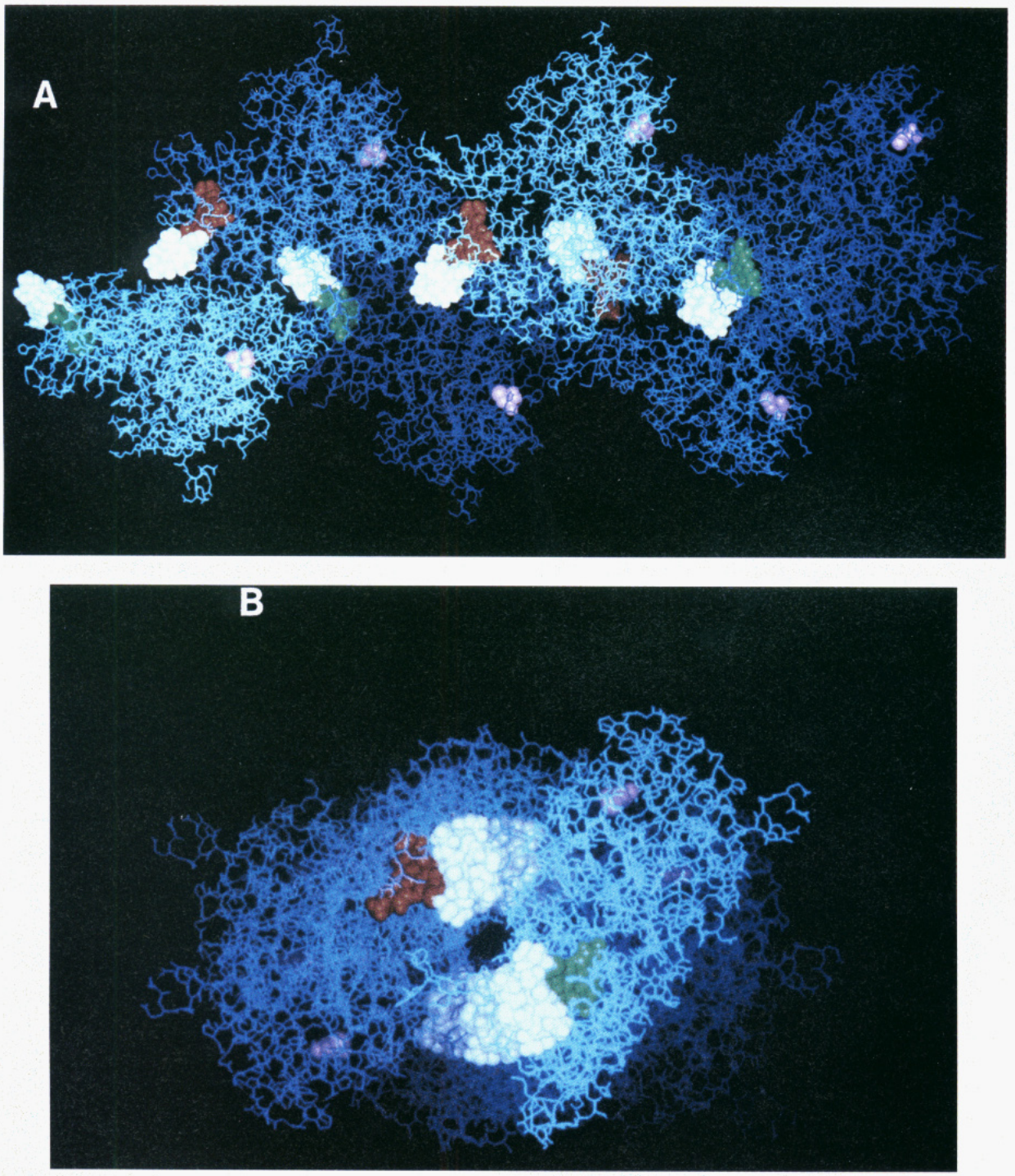

FIGURE 6: (A) Atomic structure of a six-actin monomer stretch of the F-actin filament in its complex with phalloidin (Lorenz et al., 1993). The FITC (green) and TRITC (red) groups and cysteine-374 (purple) were incorporated into the structure by Frank Hanakam of this Institute. The distance between the xanthine ring for adjacent actin monomers on different helices is 39.0 Å, and the corresponding distance between adjacent actin monomers along the same helix is 55.4 Å. (B) Same as (A) except the filament was viewed down the filament axis.

experimentally determined values of 36.9 and 37.2 Å. The corresponding distance between the same site along the same actin helix derived from the modified Lorenz et al. (1993) model is 55.4 Å. The R_0 value of 37.4 Å for the FITC-ph/TRITC-ph transfer pair on F-actin is ideally suited to study the proximity of phalloidin sites on adjacent helices, but it might be sensitive to transfer over the 55.4 Å distance between adjacent phalloidin sites along the same actin helix. However, we have calculated the expected transfer efficiency between adjacent phalloidin fluorophores along the same actin helix as only 0.08, which would be difficult to resolve from the high transfer efficiency between adjacent phalloidin molecules on opposite actin helices.

Quantitative FRETIM. FRETIM was performed on actin filaments using the in vitro motility assay as described in the Materials and Methods section. FRET between the two fluorescent phalloidins colabeled (1:1) on single filaments using 450−480 nm excitation is easily seen by eye using a fluorescence microscope based observation. Imaging a field containing colabeled filaments and the two controls, namely, filaments labeled with only FITC-ph and filaments labeled with only TRITC-ph, permits a quantitative analysis of FRET

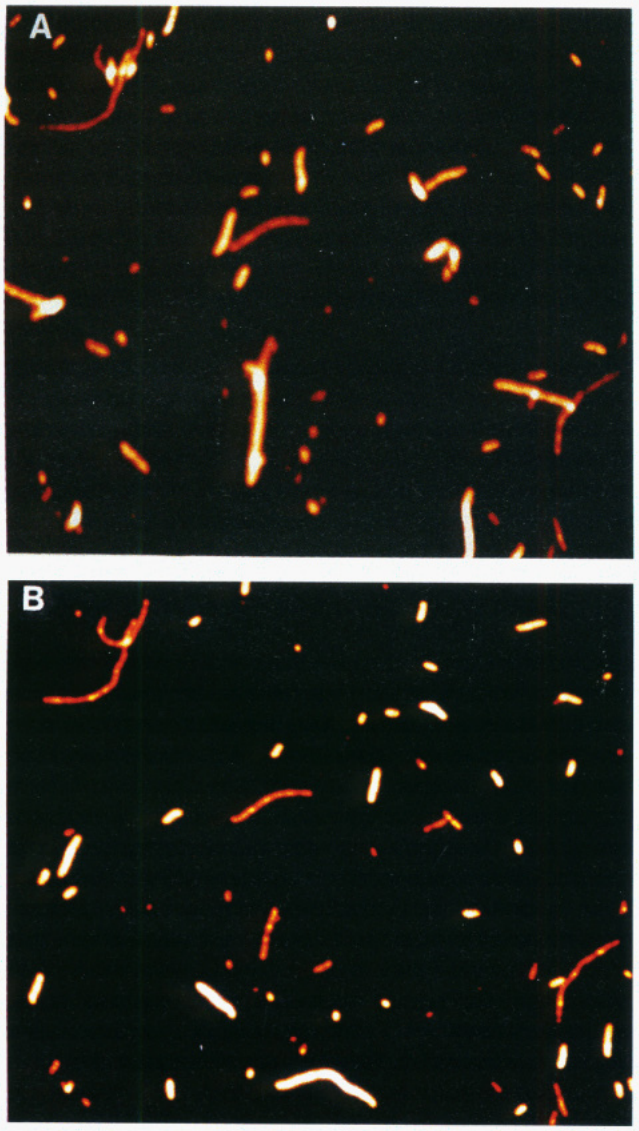

FIGURE 7: FRETIM of FITC-ph-labeled F-actin filaments, FITC-ph/TRITC-ph-labeled F-actin filaments, and TRITC-ph-labeled F-actin filaments on a surface of HMM. (A) Emission collected between 515 and 565 nm with an excitation wavelength of 450−480 nm. Average cross-section intensities were measured and used in a calculation of the efficiency of FRET. (B) Same field as (A) except excitation was 546 nm and emission beyond 580 nm to identify TRITC-ph-labeled filaments and FITC-ph/TRITC-ph-labeled filaments in the image field.

within single filaments. Thus with FITC excitation and observation of the emission using a filter that mainly collects FITC emission (515−565 nm), two types of filament were resolved (Figure 7A) and quantified for FRET as described below. A second image using TRITC excitation and mainly TRITC emission (Figure 7B) was used to assign, by comparative analysis with the previous image, the identity of the fluorophores in each filament. The efficiency of FRET for pure FITC-ph-labeled filaments and for FITC-ph/TRITC-ph-colabeled filaments was calculated using the average cross-sectional intensity per micron following localized background subtraction (Figure 7A). After normalization of the FITC-ph concentration on the filament, the average transfer efficiency found for six filaments (>3 μm) was 45%: a statistical factor of 1.25 was employed to account for the population of FITC-ph on the filament not having an adjacent TRITC-ph acceptor, leading to a revised E_t of 0.55 $\pm$ 0.02. Assuming the same quantum yield, refractive index K^2, and fluorescence lifetime for FITC-ph on actin filaments as we obtained in solution studies, a transfer efficiency of 0.55 ($k_t = 8.55 \times 10^8$ s^{-1}) was found leading to a distance between adjacent phalloidin binding sites of 36.2 Å. Considering the number of FRET pairs involved this determination, the calculated distance is remarkably similar to the solution-based measurements. ATP was added to the in vitro motility chamber to initiate sliding. The efficiency of FRET calculated for these motile filaments using a frame-by-frame analysis was similar ($E_t \sim 0.5-0.52$) to that found in the rigor complex.

Final qualitative proof that colabeled phalloidin undergoes FRET on filaments was demonstrated by recording the emission spectrum of an image field containing several tens of either FITC-ph- or FITC-ph/TRITC-ph-labeled filaments on a surface of HMM, which showed the presence of sensitized emission from TRITC-ph upon FITC excitation (data not shown).

DISCUSSION

An appreciation of how the physical properties and different structural forms of F-actin filaments are exploited to meet its cellular functions requires investigations of not only the static structure of F-actin but also its structure and structural dynamics in vitro and in vivo. FRET and fluorescence polarization techniques are well suited to study changes in the structure and structural dynamics of proteins. In this study we have shown that the phalloidin binding site of F-actin can be used to study proximity relationships between adjacent actin monomers in the filament in solution and on single filaments bound to HMM. A key factor in these studies is labeling actin filaments with fluorescent phalloidin, which offers several advantages over covalent modification of actin monomers which include (1) a single, saturatable, high-affinity binding site with a long off-rate; (2) no adverse effect on the structure of the actin monomer or filaments, cf. extrinsically labeled probes; (3) a binding site located at the interface of three monomers making it sensitive to changes in subunit conformation and this site is closer to the helix axis than extrinsic labeling sites; and (4) fluorescent phalloidin derivatives used extensively to label actin filaments in living cells and to visualize single actin filaments in the in vitro motility assay. For F-actin filaments in solution we measured a distance between adjacent phalloidin binding sites on opposite actin helices of 37.2 Å using steady-state spectral analysis and 36.9 Å using a time-resolved fluorescence analysis. Both values are in excellent agreement with the distance measured from the atomic structure (39 Å). The distance between adjacent phalloidin sites along the same actin helix of 55.4 Å is too long to probe with the donor−acceptor system employed in this study. The fluorophore attachment site of phalloidin has a radial coordinate (Taylor et al., 1981) of 14.5 Å, which makes this location an ideal reference position to probe proximity relationships between actin monomers and side-binding ABPs.

One of the major challenges in cell motility research is to understand at the molecular level how motile cells utilize a regiospecific assembly and disassembly of actin filaments and their associated protein to produce the force necessary to extend the cell membrane (Wang, 1984; Theriot & Mitchison, 1991). Quantitative investigation of the structural

properties of actin filaments in such a complex environment is perhaps best studied by imaging changes in the distance between two sites on adjacent monomers using FRET or by imaging the structural dynamics of fluorescent actin filaments using FPIM (Yan-Marriott and Marriott, in preparation). Quantitative FRETIM investigations which rely on measuring the decrease in donor quantum yield in the presence of acceptor are quite reliable and easily made in the microscope providing the donor emission of the sample can be measured in the same field as the sample containing the donor–acceptor pair or by measuring the sample image in terms of the fluorescence lifetime. We have shown these conditions are satisfied using the in vitro motility assay. Postacquisition analysis of the image field permits a direct comparison of the relative quantum yield of the FITC-ph in the absence and presence of acceptor (TRITC-ph).

The most convenient method to perform quantitative FRETIM is to measure the decrease in the relative quantum yield of the donor emission of single filaments in the presence of the TRITC-ph acceptor. The calculated distance between phalloidin sites on single filaments bound to HMM of 36.2 Å is statistically similar to that found in solution studies. No significant difference in this distance was found for actin filaments sliding on HMM following addition of ATP (data not shown), which suggests that gross structural rearrangements of the actin filament structure (Schutt et al., 1993) are not part of the actin–myosin chemo-mechanotransduction mechanism.

FRETIM was also performed by collecting, in real time, the FITC-ph and TRITC-ph emission images from single filaments. This technique can be used in a quantitative manner, but for most of our applications it is used to qualitatively demonstrate FRET, especially for nonstationary samples such as sliding actin filaments or motile cells.

Together these microscope studies have shown how quantitative FRET can be made on filaments on the order of 1 μm or about 200 FITC-ph/TRITC-ph pairs, in real time with an accuracy approaching that of solution-based spectral studies.

The spatial information available on molecular distance, using FRETIM, and the spatial information of molecular orientation, using FPIM (Kinosita et al., 1991; Yan-Marriott and Marriott, in preparation), are now being combined to provide a powerful technique to obtain new information of ABP interactions on reconstituted single actin filaments both in rigor and during ATP-dependent motility. This powerful combination of techniques is also being used to discover whether substoichiometric binding of ABPs to actin filaments leads to local structural changes in the filament. Previous studies using light microscopy and electron microscopy studies have revealed differences in the structure and properties of actin filaments through the length of the lamellipodium (Wang, 1984; Theriot & Mitchison, 1991; Small et al., 1993). FRETIM of microinjected FITC–actin and TRITC–actin in motile fibroblasts might reveal if there are any major structural changes in the actin filament structure in these different areas of the lamellipodium.

ACKNOWLEDGMENT

The authors thank Prof. Peter Fromhertz and Martin Leonhard for performing fluorescence lifetime measurements, Dr. Frank Hanakam for help with molecular modeling and useful discussions, and the K. Kolmes laboratory for making available the model of the F-actin filament over the internet.

REFERENCES

Anderson, S. R., & Weber, G. (1969) *Biochemistry 8*, 371–377.
Barden, J. A., Miki, M., Hambly, B. D., & Dos Remedios, C. G. (1987) *Eur. J. Biochem. 162*, 583–588.
Borejo, J., & Burlaca, S. (1994) *Biophys. J. 66*, 1319–1327.
Fairclough, R. H., & Cantor, C. R. (1978) *Methods Enzymol. 48*, 347–380.
Förster, T. (1948) *Ann. Phys. 9*, 21–33.
Gordon, D. J., Yang, Y.-Z., & Korn, E. D. (1976) *J. Biol. Chem. 251*, 7474–7479.
Holmes, K. C., Popp, D., Gebhard, W., & Kabsch, W. (1990) *Nature (London) 347*, 44–49.
Huang, Z., Haughland, R. P., You, W., & Haughland, R. P. (1991) *Anal. Biochem. 200*, 199–205.
Janmey, P. A., Hvitt, S., Oster, G. J., Lamb, J., Stossel, T. P., & Hartwig, J. H. (1990) *Nature (London) 347*, 95–98.
Kabsch, W., Mannertz, H., Suck, G., Pai, E., & Holmes, K. C. (1990) *Nature (London) 347*, 37–43.
Kasprzrak, A. A., Takashi, R., & Morales, M. F. (1988) *Biochemistry 27*, 4512–4522.
Kinosita, K., Jr., Itoh, H., Ishiwata, S., Hirano, K. T., Nishizuka, K., & Hayakawa, T. (1991) *J. Cell Biol. 116*, 67–73.
Kron, S. J., Toyoshima, Y. Y., Uyeda, T. P. P., & Spudich, J. A. (1991) *Methods Enzymol.*, 399–417.
Lorenz, M., Popp, D., & Holmes, K. C. (1993) *J. Mol. Biol. 234*, 826–836.
Marriott, G., Zechel, K., & Jovin, T. M. (1988) *Biochemistry 27*, 6214–6220.
Miki, M., O'Donoghue, S. I., & Dos Remedios, C. G. (1992) *J. Muscle Res. Cell Motil. 13*, 132–145.
Moens, P. J. D., Yee, J. D., & Dos Remedios, C. G. (1994) *Biochemistry 33*, 13102–13108.
Pardee, J. D., & Spudich, J. A. (1982) *Methods Enzymol. 85*, 164–181.
Schutt, C. E., Myslik, J. C., Rozycki, M. D., Goonsekere, N., & Lindberg, U. (1993) *Nature (London) 365*, 810–816.
Small, V., Rohlfs, A., & Herzog, M. (1993) in *Cell Behaviour: Adhesion and Motility. SEB Symposium No. 47* (Jones, G., Wigley, C., & Warn, R., Eds.) Company of Biologists, Cambridge, U.K.
Spudich, J. A., & Watt, S. (1971) *J. Biol. Chem. 246*, 4866–4871.
Taylor, D. L., Riedler, J., Spudich, J. A., & Stryer, L. (1981) *J. Cell Biol. 89*, 362–367.
Theriot, J. A., & Mitchison, T. J. (1991) *Nature (London) 352*, 126–131.
Waggoner, A., deBiasio, R., Conrad, P., Bright, G. R., Ernst, L., Ryan, K., Nederlof, M., & Taylor, D. L. (1989) *Methods Cell Biol. 29*, 449–478.
Wang, Y.-L. (1984) *J. Cell Biol. 99*, 1478–1485.
Wülf, E., Deboben, A., Bautz, F. A., Faulstich, H., & Wieland, Th. (1979) *Proc. Natl. Acad. Sci. U.S.A. 76*, 4498–4502.
Xue, F.-W., Lemasters, J. J., & Herman, B. (1992) *Bioimaging 1*, 30–37.

BI950379F